EDGE ARTICLE

Check for updates

Chemiluminescent duplex analysis using phenoxy-1,2-dioxetane luminophores with color modulation†

Sara Gutkin, Rozan Tannous, Qais Jaber, Micha Fridman and Doron Shabat [ID] *

Multiplex technology is an important emerging field, in diagnostic sciences, that enables the simultaneous detection of several analytes in a single sample. The light-emission spectrum of a chemiluminescent phenoxy-dioxetane luminophore can be accurately predicted by determining the fluorescence-emission spectrum of its corresponding benzoate species, which is generated during the chemiexcitation process. Based on this observation, we designed a library of chemiluminescent dioxetane luminophores with multicolor emission wavelengths. Two dioxetane luminophores that have different emission spectra, but similar quantum yield properties, were selected from the synthesized library for a duplex analysis. The selected dioxetane luminophores were equipped with two different enzymatic substrates to generate turn-ON chemiluminescent probes. This pair of probes exhibited a promising ability to act as a chemiluminescent duplex system for the simultaneous detection of two different enzymatic activities in a physiological solution. In addition, the pair of probes were also able to simultaneously detect the activities of the two enzymes in a bacterial assay, using a blue filter slit for one enzyme and a red filter slit for the other enzyme. As far as we know, this is the first successful demonstration of a chemiluminescent duplex system composed of two-color phenoxy-1,2-dioxetane luminophores. We believe that the library of dioxetanes presented here will be beneficial for developing chemiluminescence luminophores for multiplex analysis of enzymes and bioanalytes.

Multiplex technology is an important emerging field and a powerful analytical tool for the simultaneous detection of several analytes in a single sample.[1,2] This technique is immensely valuable since it can monitor the activity of multiple enzymes or analytes in real-time and offer information regarding complex biological processes at a level of detail that is beyond the reach of single analyte imaging.[3] In addition, the economy of analyzing more than one species per sample is an obvious advantage for commercial analytical laboratories.[4] Thus, reagents, solvents, time, and space can be reduced by multiplexing. Instead of one instrument for one analyte and several instruments for several single analytes, one analysis can be used for several species per sample. The cost of laboratory space, personnel, running instrumentation, and consumables are reduced. Furthermore, new analytical approaches can be investigated, because combining sets of analytes provides more information for solving a defined analytical problem.[5] While a variety of fluorescence-based scaffolds for sensing multiple targets were comprehensively studied,[6–18] multiplex examples

based on chemiluminescent dyes are rarely described and are regularly limited for immunoassays.[17,18] Thus, it remains a challenge to develop a rapid, simple, and effective chemiluminescent platform for the simultaneous detection of multiple analytes in a single sample.

Chemiluminescent probes, composed of phenoxy-adamantyl-1,2-dioxetane luminophores, can be modularly equipped with various protecting groups in order to trigger their chemiexcitation pathway.[19–23] Thus, specific responsive groups can be tailored as triggering substrates for reaction with the analyte of choice. Several years ago, our group discovered that the incorporation of an electron-withdrawing group (EWG) as a substituent at the *ortho* position of phenoxy-adamantyl-1,2-dioxetane prevents water-mediated quenching of the excited intermediate and amplifies the light-emission intensity of the chemiluminescent luminophore by up to 3000-fold (Fig. 1A).[24] Importantly, this groundbreaking development enabled the use of our chemiluminescent luminophores as a single-component probe with no required additives. Numerous research groups worldwide, including ours, took advantage of an *ortho*-substituted phenoxy-adamantyl-1,2-dioxetane luminophore to develop useful chemiluminescent probes for use in cells and *in vivo* assays.[25–48]

The electronic molecular structure of the EWG substituent can directly affect the light emission wavelength of the

Department of Organic Chemistry, School of Chemistry, Raymond and Beverly Sackler Faculty of Exact Sciences, Tel-Aviv University, Tel Aviv 69978, Israel. E-mail: chdoron@tauex.tau.ac.il; Tel: +972 3 640 8340

† Electronic supplementary information (ESI) available. See DOI: https://doi.org/10.1039/d3sc02386a
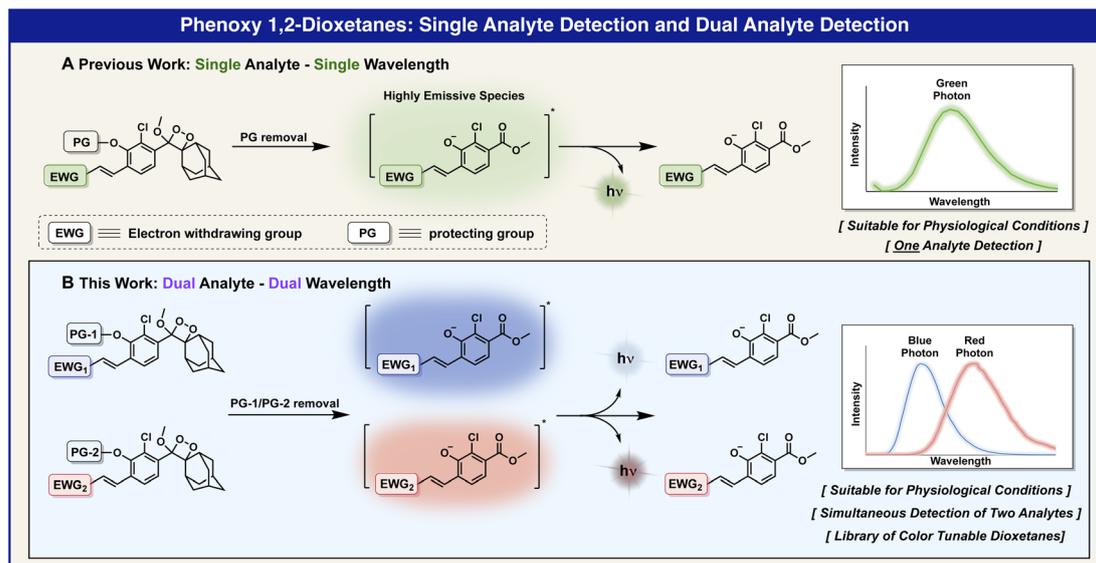
Fig. 1   General presentation of two-color chemiluminescent luminophores for a duplex analysis.

chemiluminescent dioxetane luminophore (Fig. 1B). Therefore, the incorporation of different EWG substituents at the *ortho* position of the phenoxy-dioxetane scaffold provides chemiluminescent luminophores with different colors.[23] Here we report a practical two-color chemiluminescent duplex system, based on phenoxy-1,2-dioxetane luminophores for simultaneous detection of two analytes.

The light-emission wavelength of a chemiluminescent phenoxy-dioxetane luminophore can be accurately predicted by determining the fluorescence-emission wavelength of its corresponding benzoate species, which is generated during the chemiexcitation process (Fig. 2A). Thus, we initially sought to screen a library of benzoates, substituted with various EWGs, and to use the obtained data to select a suitable pair of phenoxy-dioxetane luminophores with different light-emission wavelengths, in order to prepare chemiluminescent probes for duplex analysis.

The molecular structures of 15 benzoates, bearing various substituents, positioned *ortho* to the phenol are presented in Fig. 2B. The synthesis of these benzoate derivatives was achieved as described in the ESI.† In general, reagents bearing various EWGs were condensed with an appropriate aldehyde to afford their corresponding benzoate derivatives. The benzothiazole benzoate E490 was obtained *via* a reaction of the aldehyde with 2-amino-thiophenol and the hydroxy coumarin benzoate A460 was prepared *via* thermal decomposition of its corresponding dioxetane derivative. All benzoates exhibit fluorescence with wide-ranging emission wavelengths from 460 nm to 710 nm.

The optical spectra and properties were measured for the fluorescent benzoates (A–O) and the obtained data are presented in Table 1. Benzoate A460 has a molecular core that is based on 7-hydroxy-coumarin, benzoate J610 has an *ortho* substituent that exists in the Green Fluorescent Protein (GFP) dye and benzoate L710 has an *ortho* substituent inspired by the

dicyanomethylene-4H-chromene NIR fluorescent dye. The other benzoates have varied lengths of conjugated *ortho* substituents or varied electron withdrawing groups.

In general benzoates with shorter emission wavelengths exhibited higher fluorescence quantum yield. Since benzoates with red to far-red emission wavelengths have molecular structures of elongated π-electron systems, which are less rigid, they are susceptible to a higher degree of non-radiative decay in their excited state. The elongation of the π-electron conjugation resulted in a longer emission wavelength of about 50 nm for each additional double bond.

In order to confirm that the emission wavelengths of the fluorescent benzoates match the emission wavelengths of their corresponding chemiluminescent phenoxy 1,2-dioxetane luminophores, we next synthesized the corresponding phenoxy-adamantyl-1,2-dioxetane derivatives (see the ESI†). The molecular structures and the emission colors of these chemiluminescent phenoxy-adamantyl-1,2-dioxetane luminophores are presented in Fig. 3. In general, most of the compounds were synthesized by Wittig or Knoevenagel condensations of an *ortho*-substituted aldehyde with various reagents bearing EWGs. These transformations afforded enolether intermediates that were subsequently oxidized by singlet oxygen to produce their corresponding 1,2-dioxetanes. The synthesis of benzothiazole dioxetane E490 was achieved by condensation of an *ortho*-aldehyde enolether with 2-amino-thiophenol, followed by singlet oxygen oxidation, and the synthesis of coumarin dioxetane A460 was performed as reported earlier.[49] The synthesized 1,2-dioxetanes were obtained in moderate to high yields and presented decent thermal stability, with little to no decomposition at all to the corresponding benzoates after long storage periods in a solid form or in stock solutions in DMSO at −20 °C (ESI, Fig. S8†). A visual demonstration of the phenoxy-1,2-dioxetanes chemiexcitation is shown in Fig. 3.
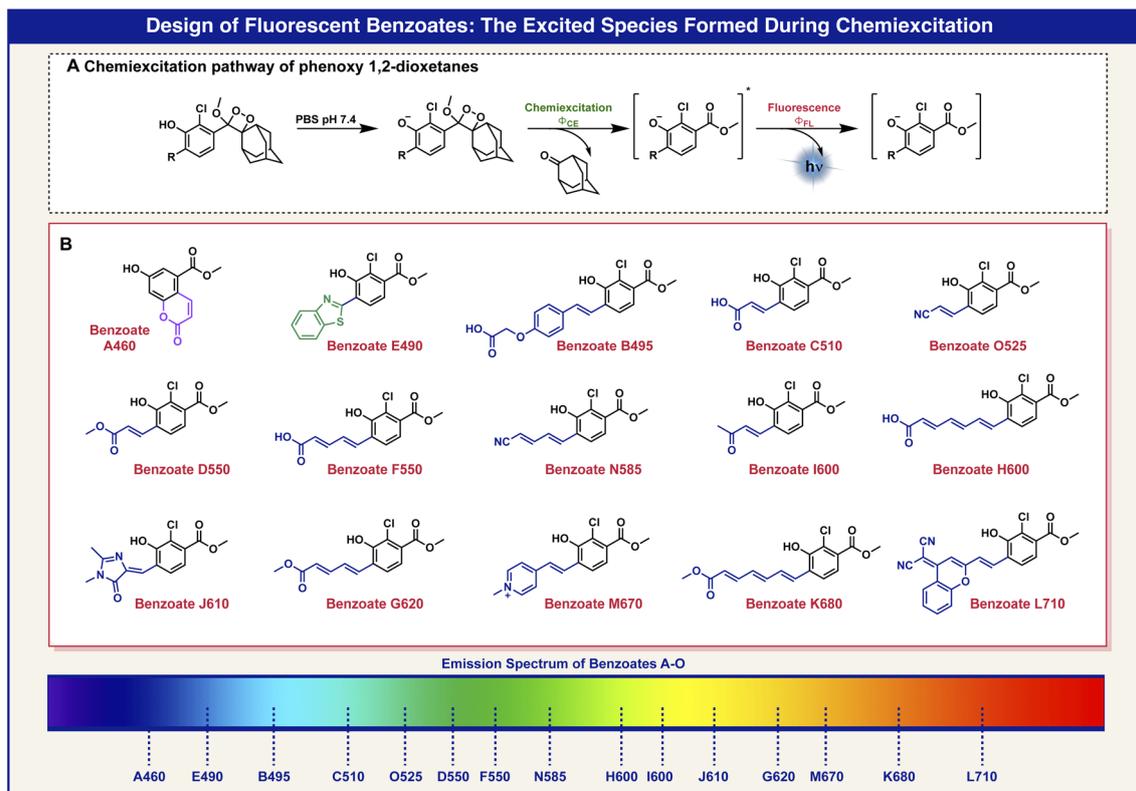
Fig. 2 (A) Chemiluminescent disassembly pathway of 1,2-dioxetane. (B) Molecular structures of various benzoate derivatives with wide-ranging emission wavelengths.

Next, we measured the chemiluminescence properties of the dioxetane luminophores, including light-emission spectra, the half-life ($T_{1/2}$) of the light emission profile, chemiluminescence quantum yield and brightness. The chemiexcitation of the phenoxy dioxetanes was triggered by deprotonation of the phenolic hydrogen under physiological conditions in PBS 7.4. The obtained data are summarized in Table 2.

Predictably, the chemiluminescent emission spectra of the dioxetane luminophores overlapped the fluorescent emission spectra of their corresponding benzoates (ESI, Fig. S3†). The chemiexcitation of the phenoxy-dioxetanes resulted in light emission decay kinetic profiles with different $T_{1/2}$. The chemiluminescent quantum yields for all dioxetane luminophores were calculated using dioxetane C510 as a reference.[50] The brightness of the chemiluminescent luminophores was determined by the intensity of light emission per unit of time. Therefore phenoxy-dioxetanes, which exhibited faster light emission decay profiles (shorter $T_{1/2}$), had higher brightness values. For example, dioxetane B495 exhibited a $T_{1/2}$ value of 3.4 s and a chemiluminescent quantum yield of 0.58%, making it the brightest dioxetane in our array. Dioxetanes A460 and E490 exhibited the longest $T_{1/2}$ values, 16 h and 10.3 h respectively. Therefore, their light emission intensity per time interval was substantially lower. Such circumstances result in a low brightness value for these dioxetanes, despite their high chemiluminescent quantum yield (55% and 20% respectively).
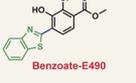
In order to enable the simultaneous detection of several analytes in a single sample, a chemiluminescent multiplex system should be composed of 1,2-dioxetane luminophores, each emitting at a different wavelength. Importantly the emission bands of the selected luminophores should be with similar intensities and with a sufficient wavelength distance one from the other, which facilitates adequate resolution (Fig. 4A). To validate the feasibility of such a chemiluminescent multiplex system, we sought to demonstrate a dual-color two-enzyme detection duplex.

Based on the optical properties of the benzoates and dioxetanes presented in Tables 1 and 2, phenoxy-dioxetanes B495 and G610 were selected as a suitable luminophore-pair for a duplex system (Fig. 4B). The chemiluminescence maximum emission wavelength gap of these dioxetanes is more than 100 nm (495 nm and 610 nm respectively) and their chemiluminescence quantum yields are similar (0.58% and 0.50% respectively). The $T_{1/2}$ value difference of dioxetane B495 and G610 is not ideal (3.4 s and 31.2 s respectively); however, this variance can be compensated for by measuring the light-emission signals at a specific time slot.

Phenoxy-dioxetanes luminophores G610 and B495 were masked with two different enzymatic substrates to form the chemiluminescent turn-ON probes, DPLX-1 and DPLX-2 (Fig. 4C). Dioxetane luminophore G610 was equipped with a triggering substrate aimed for activation by the reductase enzyme NQO1 (probe DPLX-1) and dioxetane luminophore

Table 1 Molecular structures and optical parameters of fluorescent benzoates with different *ortho* substituents. Benzoates A−O [100 μM] in PBS [100 mM], pH 7.4, and 10% DMSO. Relative intensity (fluorescence quantum yield) was measured by exciting each benzoate by the maximum absorbance value. The extinction coefficient was determined by measuring the absorbance for different concentrations and generating a calibration curve for each benzoate. *Measurements were conducted in pH 11, carbonate buffer, due to the high pK_a value of this phenol

Spectroscopic Parameters of Fluorescent Benzoates in PBS, pH 7.4				
Benzoate	Absorption Spectra	Emission Spectra	$\varepsilon_{\lambda,max}$ [M^{-1}cm^{-1}]	Φ_{FL}
Benzoate-A460		460 nm	$\varepsilon_{380} = 13666$	48.78*
Benzoate-E490	pH 11	490 nm	$\varepsilon_{400} = 11000$*	37.54*
Benzoate-B495	pH 11	495 nm	$\varepsilon_{370} = 4666$*	4.81*
Benzoate-C510		510 nm	$\varepsilon_{380} = 4333$	8.78
Benzoate-O525		525 nm	$\varepsilon_{400} = 6000$	12.88
Benzoate-D550		550 nm	$\varepsilon_{400} = 6666$	5.20
Benzoate-F550		550 nm	$\varepsilon_{400} = 7000$	5.39
Benzoate-N585		585 nm	$\varepsilon_{410} = 5333$	2.77
Benzoate-I600		600 nm	$\varepsilon_{415} = 5333$	0.28
Benzoate-H600	pH 11	600 nm	$\varepsilon_{415} = 8333$*	1.07*
Benzoate-J610		610 nm	$\varepsilon_{460} = 6000$	0.41
Benzoate-G620		620 nm	$\varepsilon_{405} = 9666$	1.23
Benzoate-M670		670 nm	$\varepsilon_{460} = 11666$	0.29
Benzoate-K680		680 nm	$\varepsilon_{420} = 10666$	0.46
Benzoate-L710		710 nm	$\varepsilon_{400} = 17666$	0.32
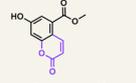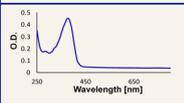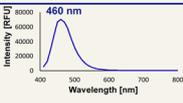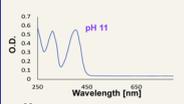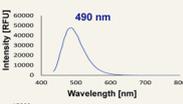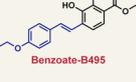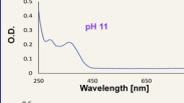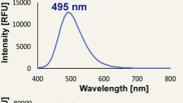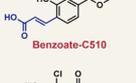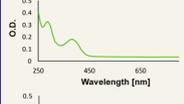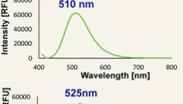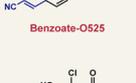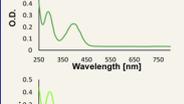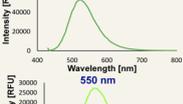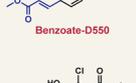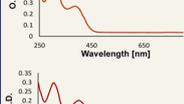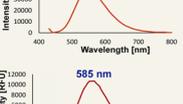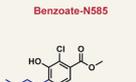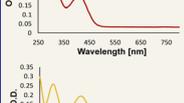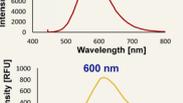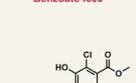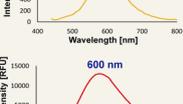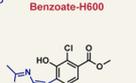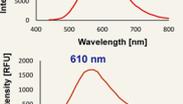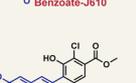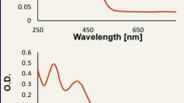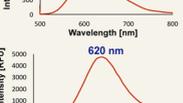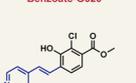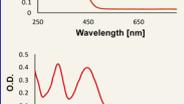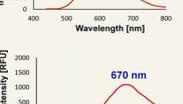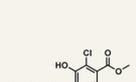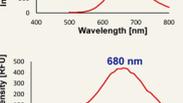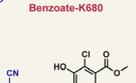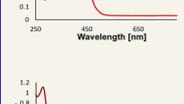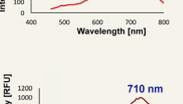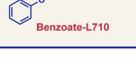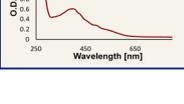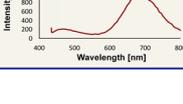
Fig. 3 Molecular structures of various phenoxy–adamantyl-1,2-dioxetane luminophores with wide-ranging emission wavelengths, and a demonstration of phenoxy-1,2-dioxetane activation using saturated sodium bicarbonate solution.
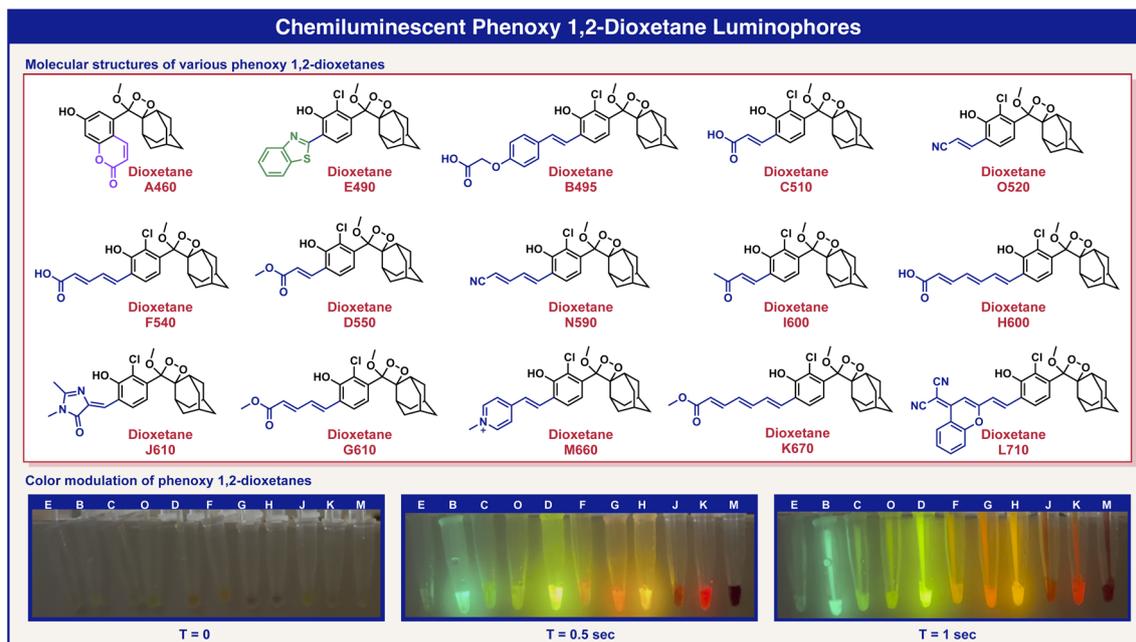
B495, with a triggering substrate aimed for activation by alkaline phosphatase (probe DPLX-2). Since dioxetane G610 exhibited poorer aqueous solubility than dioxetane B495, its methyl-ester functional group was replaced with a dicarboxylic acid function that is more water-soluble (see the molecular structure of probe DPLX-1 in Fig. 4C). This modification did not affect the optical properties of dioxetane luminophore G610 (ESI, Fig. S9†).

Expectedly, probes DPLX-1 and DPLX-2 exhibited a substantial turn-ON response to NQO1 and to alkaline phosphatase respectively, displaying a typical kinetic chemiluminescence profile of an increase and decay. The light emission spectrum of probe DPLX-1 (Fig. 4C, red), in the presence of NQO1, generates a sufficient distance in λ_{max} from the light emission spectrum of probe DPLX-2, in the presence of alkaline phosphatase (Fig. 4C, blue). The light emission spectrum generated by the simultaneous activation of both probes by the two enzymes also shows two partially resolved emissions maxima (Fig. 4C, green).

To evaluate the ability of probes DPLX-1 and DPLX-2 to serve as a suitable pair for a duplex analysis, their chemiluminescence light emissions were measured using a set of two different filters. Since the activation of probe DPLX-1 resulted in a maximum emission wavelength of 610 nm, with an emission band from 495 nm to 750 nm, we used a wavelength of 650 nm for the red filter. On the other hand, since the activation of probe DPLX-2 resulted in a maximum emission wavelength of 495 nm, with an emission band from 430 nm to 620 nm, we used a wavelength of 470 nm for the blue filter. Such a selection of filters will maximize the amount of light gathered for a specific probe and minimize the light leakage to the emission band of the other probe.

Probes DPLX-1 and DPLX-2 were incubated in the presence and absence of NQO1 and alkaline phosphatase and the light-emitted signal was measured using the filters described above. The obtained data are presented in Fig. 4. Using the red filter, probe DPLX-1 exhibits a strong light emission signal in response to NQO1, which is 310-fold higher than the signal produced in the absence of the enzyme. Similarly, using the blue filter, probe DPLX-2 also exhibits a strong light emission signal in response to alkaline phosphatase, which is 1166-fold higher than the signal produced in the absence of the enzyme. Both probes show only minimal light leakage in the other filter.

Next, we measured the concurrent turn-ON response of a 1 : 1 mixture of probes DPLX-1 and DPLX-2, in the presence and absence of NQO1 and alkaline phosphatase, using the blue or the red filters (right, Fig. 4D). Intriguingly, the chemiluminescence light emission profile of each probe was not affected by the presence of the other, nor by the intensity or the light emission rate (overlay graphs are presented in the ESI, Fig. S11†). In addition, the S/N values in the simultaneous measurement were similar to the S/N values observed in the individual measurements (S/N values of 310 and 910 respectively). The obtained data show that the selected pair of probes produce well-separated two-color emission bands with high detection sensitivity towards their enzymes.

The ability of probes DPLX-1 and DPLX-2 to provide straightforward real-time analyte detection has prompted us to explore their performance for a dual-color duplex analysis in a bacterial assay. Three bacterial strains that are known to express either NQO1, alkaline phosphatase, or both were selected for this study. *Staphylococcus aureus* (ATCC 35556) is a bacterium that expresses both the enzymes NQO1 and alkaline phosphatase, *Streptococcus mutans* (ATCC 35668) is a bacterium that expresses the enzyme NQO1, and *Streptococcus*

Table 2 Molecular structures and chemiluminescence parameters of 1,2-dioxetanes with different *ortho* substituents. Dioxetanes A–O [1 μM] in PBS [100 mM], pH 7.4, and 10% DMSO. Relative intensity was determined for each dioxetane in comparison to literature values of known dioxetanes, and brightness was determined as the total light emitted divided by the chemiexcitation rate in minutes

Spectroscopic Parameters of Phenoxy-1,2-Dioxetane Chemiluminescent Luminophores in PBS, pH 7.4					
Phenoxy 1,2-dioxetane	Emission Spectra	$\lambda_{max}CL$ [nm]	$T_{1/2}$	Relative Brightness	Φ_{CL} %
Dioxetane A460		460 nm	16 hours	1	55
Dioxetane E490		490 nm	10.3 hours	0.70	20
Dioxetane B495		495 nm	3.4 seconds	480	0.58
Dioxetane C510		510 nm	1.6 minutes	245	9.8
Dioxetane O520		520 nm	20 minutes	41	20
Dioxetane D550		550 nm	10.5 minutes	16	4.8
Dioxetane F540		540 nm	15.6 seconds	206	1.9
Dioxetane N590		590 nm	2 minutes	39	1.1
Dioxetane I600		600 nm	13.5 minutes	0.85	0.42
Dioxetane H600		600 nm	3.3 seconds	65	0.14
Dioxetane J610		610 nm	11.9 minutes	0.25	0.073
Dioxetane G610		610 nm	31.2 seconds	8.3	0.5
Dioxetane M660		660 nm	5 minutes	0.24	0.13
Dioxetane K670		670 nm	18 seconds	1.2	0.012
Dioxetane L710		710 nm	17 minutes	0.61	0.38
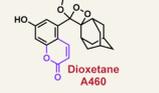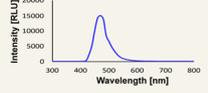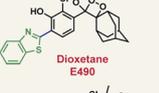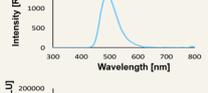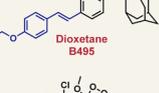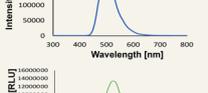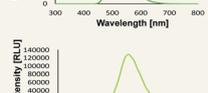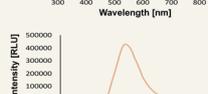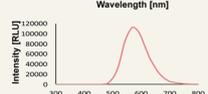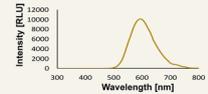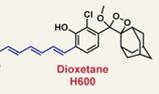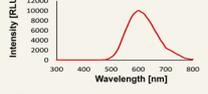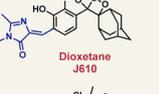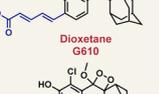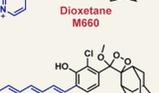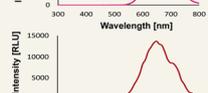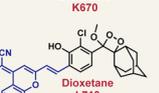
Selection and Evaluation of A Chemiluminescent Duplex Pair for Enzymatic Assay

A. General presentation of a chemiluminescent duplex system

B. Selection of a suitable duplex system

	λ_{max}CL [nm]	$T_{1/2}$	ϕ_{CL}(H2O)
Dioxetane B495	495 nm	3.4 seconds	0.58%
Dioxetnae G610	600 nm	30 seconds	0.50%

[Similar ϕ_{CL}] [Different emission spectrum - at least 100 nm difference in λ_{max}] [Corresponding $T_{1/2}$ parameters for simultaneous monitoring]

C. Chemiluminescence emission spectra of DPLX-1 and DPLX-2

D. Simultaneous monitoring of two enzymatic procedures using a duplex system: DPLX-1 and DPLX-2

Fig. 4 (A) General scheme of a chemiluminescence duplex system for simultaneous monitoring of different analytes. (B) Molecular structures and chemiluminescent properties of the two selected luminophores for the duplex system. (C) Chemiluminescence emission spectra of DPLX-1 [100 μM] and DPLX-2 [100 μM] with NQO1 [20 μg ml^{-1}] and ALP [7.5 U ml^{-1}] in PBS 7.4, 10% DMSO, and NADH [100 μM] at 25 °C. The green curve represents the measurement of both DPLX-1 and DPLX-2 at the same well, at the same time. (D) Left: Total light emission of DPLX-1 [10μM] with and without NQO1 [20 μg ml^{-1}] in PBS 7.4, 10% DMSO, and NADH [100 μM] at 25 °C. The light emitted was measured at 470 nm and 650 nm (slit of 15 nm) and total light emission values were taken after 60 minutes of measurement. Middle: Total light emission of DPLX-2 [10 μM] with and without ALP [7.5 U ml^{-1}] in PBS 7.4 and 10% DMSO at 25 °C. The light emitted was measured at 470 nm and 650 nm (slit of 15 nm) and total light emission values were taken after 60 minutes of measurement. Right: Total light emission of DPLX-1 [10 μM] and DPLX-2 [10 μM] with and without NQO1 [20 μg ml^{-1}] and ALP [7.5 U ml^{-1}] in PBS 7.4, 10% DMSO, and NADH [100 μM] at 25 °C. The light emitted was measured at 470 nm and 650 nm (slit of 15 nm) and total light emission values were taken after 60 minutes of measurement.

pyogenes (glossy) is a bacterium that expresses alkaline phosphatase.[51,52]
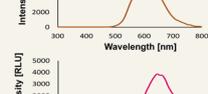
Probes DPLX-1 and DPLX-2 were incubated with the three different bacterial strains and their light emission signal was measured using blue and red filters (Fig. 5). The incubation of

the two probes with *Staphylococcus aureus* (ATCC 35556) resulted in strong signals with substantial S/N values by using both the blue filter slit and the red filter slit (Fig. 5A, left). These measurements indicate the expression of the two enzymes NQO1 and alkaline phosphatase by this bacterial strain. On the
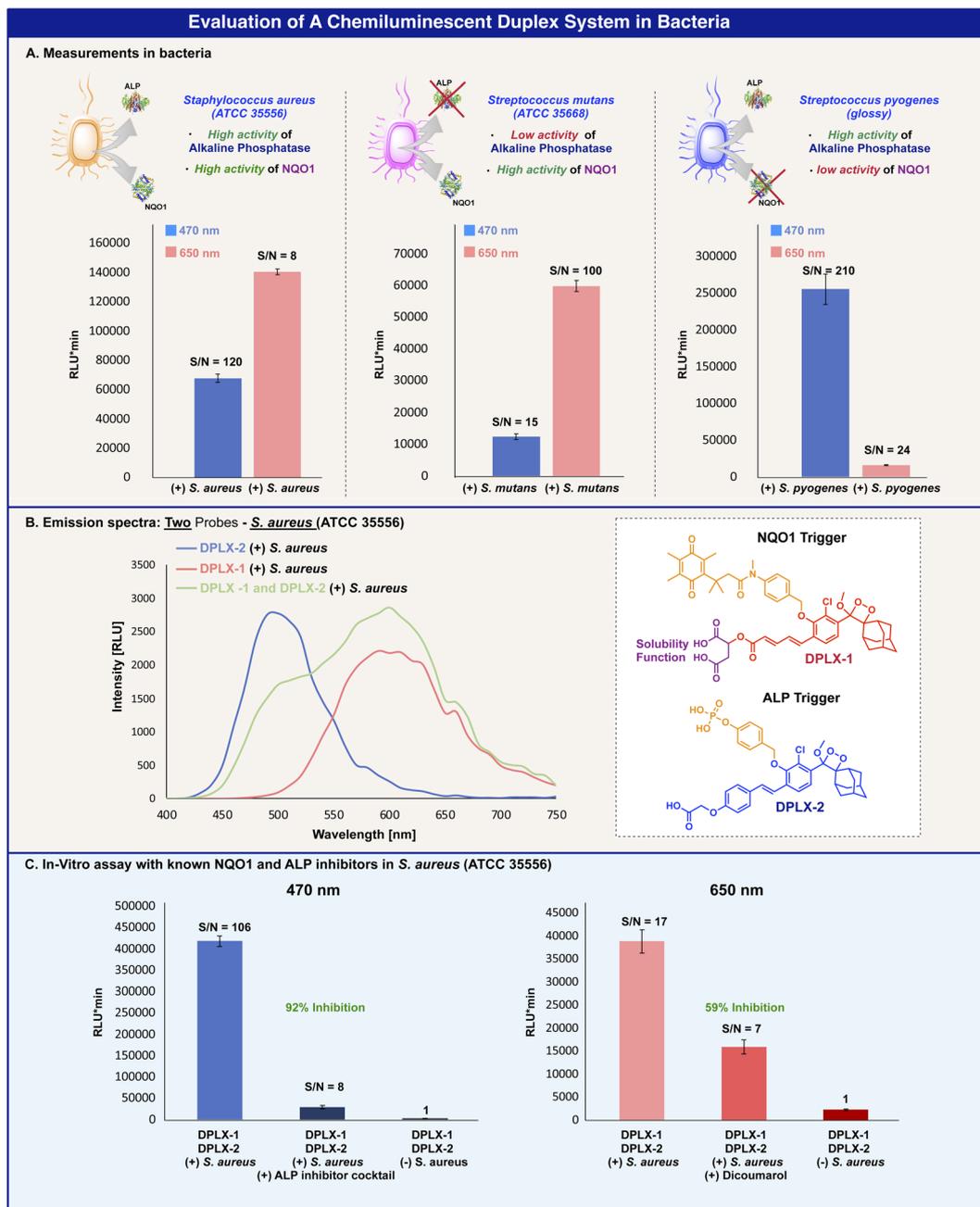
Fig. 5 (A) Total light emission of DPLX-1 [100 μM] and DPLX-2 [100 μM] with *S. aureus* (ATCC 35556) (left), *S. mutans* (ATCC 35668) (middle), and *S. pyogenes* (glossy) (right) in PBS 7.4 and 10% DMSO at 37 °C. The light emission was measured at 470 nm and 650 nm and total light emission values were taken after 20 minutes from the addition of the probes. (B) Chemiluminescence emission spectra of DPLX-1 [100 μM] and DPLX-2 [100 μM] with S. *aureus* in PBS 7.4 and 10% DMSO at 37 °C. The green curve represents the measurement of both DPLX-1 and DPLX-2 at the same well, at the same time. (C) Total light emission of DPLX-1 [100 μM] and DPLX-2 [100 μM] with *S. aureus* in the presence of ALP inhibitor cocktail (1 μL) and dicoumarol (5 eq.) in PBS 7.4 and 5% DMSO at 37 °C. The light emission was measured at 470 nm and 650 nm and total light emission values were taken 30 minutes after the addition of the probes.

other hand, the incubation of the two probes with *Streptococcus mutans* (ATCC 35668) resulted in a strong light emission signal using the red filter slit and a low signal when using the blue filter slit; indicating that this bacterial strain highly expresses the enzyme NQO1 and only slightly expresses alkaline phosphatase (Fig. 5A, middle). Similarly, the incubation of the two probes with *Streptococcus pyogenes* (glossy) resulted in a strong

light emission signal using the blue filter slit and a low signal when using the red filter slit, indicating that this bacterial strain highly expresses alkaline phosphatase and only slightly expresses the NQO1 enzyme (Fig. 5A, right).

The measurements of the full emission spectra of probes DPLX-1 and DPLX-2 in the presence of the bacterial strain (*Staphylococcus aureus* (ATCC 35556)) that expresses both

© 2023 The Author(s). Published by the Royal Society of Chemistry

enzymes, NQO1 and alkaline phosphatase, showed similar spectral patterns to the emission spectra observed with probes DPLX-1 and DPLX-2 in PBS 7.4 in the presence of the two enzymes (Fig. 5B).

To further confirm that probes DPLX-1 and DPLX-2 are specifically activated by NQO1 and alkaline phosphatase, we performed the measurements in the presence of inhibitors, dicoumarol, which is a specific inhibitor for NQO1, and a known inhibitor cocktail for alkaline phosphatase.[52]

Both probes were incubated with *Staphylococcus aureus* (ATCC 35556) and with either one of the two inhibitors and after 30 min, the chemiluminescence signal was measured using either the red or the blue filters. Indeed, a signal inhibition of 92% was observed for alkaline phosphatase using the blue filter, and a signal inhibition of 59% was observed for NQO1 using the red filter (Fig. 5C). The obtained results clearly show the feasibility of probes DPLX-1 and DPLX-2 to function as a chemiluminescence duplex system, that enables the simultaneous detection of alkaline phosphatase and NQO1 in a bacterial assay.

Fluorescence and chemiluminescence are two related optical phenomena that are based on a light emission signal. However, in contrast to fluorescence, chemiluminescence does not require irradiation by an external light source and as a result, the background signal is extremely low, and the obtained sensitivity is considerably enhanced. In *in vivo* settings, the excitation light source used in fluorescence to excite a fluorogenic dye can also excite other biomolecules present in the mammalian tissues. Such circumstances generate a substantial background signal, which significantly decreases the overall signal-to-noise ratio value of the measurement. This disadvantage is totally avoided in chemiluminescence since the excitation of the chemiluminophore occurs through a chemical reaction and no external light is required. As a result, the signal-to-noise ratio produced by chemiluminescence is much higher than that produced by fluorescence.

Several duplex and multiplex examples, that employ a fluorescent output, were reported over the last few years.[6,9,13–15] One example described a duplex system that employs one fluorescence output and one chemiluminescence output.[10] However, a duplex system with two-color chemiluminescence dioxetane luminophores was never demonstrated before. The ability to incorporate various substituents at the *ortho* position of a phenoxy-dioxetane enables us to gain control and fine-tune the emission wavelength of the dioxetane luminophores. In general, an efficient duplex system should be composed of a pair of dyes with different emission wavelengths and a sufficient spectral gap. Importantly the emission intensity should be similar for both dyes, in order to enable simultaneous detection of the turn-ON signal generated by the response of the two analytes of interest with the pair of probes. The library of dioxetane luminophores presented in Table 2 may be useful for the selection of additional colors for achieving a multiplex analysis system.

In summary, we synthesized a small library of chemiluminescent dioxetane luminophores with multicolor emission wavelengths. The emission wavelength of the chemiluminescent dioxetane could be efficiently determined by the measurement of the fluorescence emission of its corresponding benzoate byproduct. Two dioxetane luminophores that have different emission spectra, but similar quantum yield properties, were selected from the synthesized library. The selected dioxetane luminophores were equipped with two different enzymatic substrates to generate turn-ON chemiluminescent probes. This pair of probes exhibited a promising ability to act as a chemiluminescent duplex system for the simultaneous detection of two different enzymatic activities in a physiological solution. Remarkably, the pair of probes was also able to simultaneously detect the activities of the two enzymes in a bacterial assay, using a blue filter slit for one enzyme and a red filter slit for the other enzyme. As far as we know, this is the first successful demonstration of a chemiluminescent duplex system composed of two-color phenoxy-1,2-dioxetane luminophores. We anticipate that the library of dioxetanes presented here will be useful for the development of chemiluminescent probes for multiplex analysis of different analytes.

Data availability

Data supporting this article have been uploaded as ESI.†

Author contributions

S. G. and R. T. performed the synthesis and analyzed DPLX-1 and DPLX-2 assay data under the supervision of D. S. and Q. J. performed bacterial assays under the supervision of M. F. All authors contributed to the discussion and revision of the manuscript.

Conflicts of interest

There are no conflicts to declare.

Acknowledgements

References

1 A. M. Bittel, A. M. Davis, L. Wang, M. A. Nederlof, J. O. Escobedo, R. M. Strongin and S. L. Gibbs, *Sci. Rep.*, 2018, **8**, 4590.

2 M. Sauer, K. T. Han, V. Ebert, R. Muller, A. Schulz, S. Seeger, J. Wolfrum, J. Ardenjacob, G. Deltau, N. J. Marx and K. H. Drexhage, *Proc. SPIE-Int. Soc. Opt. Eng.*, 1994, **2137**, 762–774.

3 J. Y. Guo, B. Fang, H. Bai, L. M. Wang, B. Peng, X. J. Qin, L. Fu, C. H. Yao, L. Li and W. Huang, *TrAC, Trends Anal. Chem.*, 2022, **155**, 116697.

4 S. Benson, F. de Moliner, W. Tipping and M. Vendrell, *Angew. Chem., Int. Ed.*, 2022, **61**, e202204788.

5 D. Kovacs, X. Lu, L. S. Meszaros, M. Ott, J. Andres and K. E. Borbas, *J. Am. Chem. Soc.*, 2017, **139**, 5756–5767.

6 E. Pershagen and K. E. Borbas, *Angew. Chem., Int. Ed.*, 2015, **54**, 1787–1790.

7 M. A. Bray, S. Singh, H. Han, C. T. Davis, B. Borgeson, C. Hartland, M. Kost-Alimova, S. M. Gustafsdottir, C. C. Gibson and A. E. Carpenter, *Nat. Protoc.*, 2016, **11**, 1757–1774.

8 Y. Okorochenkova, M. Porubsky, S. Benicka and J. Hlavac, *Chem. Commun.*, 2018, **54**, 7589–7592.

9 R. S. Xiong, D. Mara, J. Liu, R. Van Deun and K. E. Borbas, *J. Am. Chem. Soc.*, 2018, **140**, 10975–10979.

10 P. H. Cheng, Q. Q. Miao, J. C. Li, J. G. Huang, C. Xie and K. Y. Pu, *J. Am. Chem. Soc.*, 2019, **141**, 10581–10584.

11 R. C. Brown, Z. Li, A. J. Rutter, X. Mu, O. H. Weeks, K. Smith and I. Weeks, *Org. Biomol. Chem.*, 2009, **7**, 386–394.

12 Y. Sun and J. Z. Lu, *Luminescence*, 2018, **33**, 1298–1305.

13 Z. H. Lei, C. X. Sun, P. Pei, S. F. Wang, D. D. Li, X. Zhang and F. Zhang, *Angew. Chem., Int. Ed.*, 2019, **58**, 8166–8171.

14 J. Y. Xu, L. N. Fang, M. Shi, Y. Huang, L. F. Yao, S. L. Zhao, L. L. Zhang and H. Liang, *Chem. Commun.*, 2019, **55**, 1651–1654.

15 Y. K. Yue, F. J. Huo, F. Q. Cheng, X. J. Zhu, T. Mafireyi, R. M. Strongin and C. X. Yin, *Chem. Soc. Rev.*, 2019, **48**, 4155–4177.

16 H. Fujioka, J. W. Shou, R. Kojima, Y. Urano, Y. Ozeki and M. Kamiya, *J. Am. Chem. Soc.*, 2020, **142**, 20701–20707.

17 W. C. C. Tan, S. N. Nerurkar, H. Y. Cai, H. H. M. Ng, D. D. Wu, Y. T. F. Wee, J. C. T. Lim, J. Yeong and T. K. H. Lim, *Cancer Commun.*, 2020, **40**, 135–153.

18 Y. T. Zhang, C. X. Yan, C. Wang, Z. Q. Guo, X. G. Liu and W. H. Zhu, *Angew. Chem., Int. Ed.*, 2020, **59**, 9059–9066.

19 N. Hananya and D. Shabat, *Angew. Chem., Int. Ed.*, 2017, **56**, 16454–16463.

20 S. Gnaim, O. Green and D. Shabat, *Chem. Commun.*, 2018, **54**, 2073–2085.

21 N. Hananya and D. Shabat, *ACS Cent. Sci.*, 2019, **5**, 949–959.

22 M. W. Yang, J. G. Huang, J. L. Fan, J. J. Du, K. Y. Pu and X. J. Peng, *Chem. Soc. Rev.*, 2020, **49**, 6800–6815.

23 U. Haris and A. R. Lippert, *ACS Sens.*, 2023, **8**(1), 3–11.

24 O. Green, T. Eilon, N. Hananya, S. Gutkin, C. R. Bauer and D. Shabat, *ACS Cent. Sci.*, 2017, **3**, 349–358.

25 O. Green, S. Gnaim, R. Blau, A. Eldar-Boock, R. Satchi-Fainaro and D. Shabat, *J. Am. Chem. Soc.*, 2017, **139**, 13243–13248.

26 N. Hananya, O. Green, R. Blau, R. Satchi-Fainaro and D. Shabat, *Angew. Chem., Int. Ed.*, 2017, **56**, 11793–11796.

27 M. E. Roth-Konforti, C. R. Bauer and D. Shabat, *Angew. Chem., Int. Ed.*, 2017, **56**, 15633–15638.

28 M. Roth-Konforti, O. Green, M. Hupfeld, L. Fieseler, N. Heinrich, J. Ihssen, R. Vorberg, L. Wick, U. Spitz and D. Shabat, *Angew. Chem., Int. Ed.*, 2019, **58**, 10361–10367.

29 S. Son, M. Won, O. Green, N. Hananya, A. Sharma, Y. Jeon, J. H. Kwak, J. L. Sessler, D. Shabat and J. S. Kim, *Angew. Chem., Int. Ed.*, 2019, **58**, 1739–1743.

30 S. Das, J. Ihssen, L. Wick, U. Spitz and D. Shabat, *Chem.–Eur. J.*, 2020, **26**, 3647–3652.

31 S. Gutkin, O. Green, G. Raviv, D. Shabat and O. Portnoy, *Bioconjugate Chem.*, 2020, **31**, 2488–2493.

32 M. W. Yang, J. W. Zhang, D. R. Shabat, J. L. Fan and X. J. Peng, *ACS Sens.*, 2020, **5**, 3158–3164.

33 S. Ye, N. Hananya, O. Green, H. S. Chen, A. Q. Zhao, J. G. Shen, D. Shabat and D. Yang, *Angew. Chem., Int. Ed.*, 2020, **59**, 14326–14330.

34 B. M. Babin, G. Fernandez-Cuervo, J. Sheng, O. Green, A. A. Ordonez, M. L. Turner, L. J. Keller, S. K. Jain, D. Shabat and M. Bogyo, *ACS Cent. Sci.*, 2021, **7**, 803–814.

35 S. P. Gholap, C. Y. Yao, O. Green, M. Babjak, P. Jakubec, T. Malatinsky, J. Ihssen, L. Wick, U. Spitz and D. Shabat, *Bioconjugate Chem.*, 2021, **32**, 991–1000.

36 S. Gutkin, S. Gandhesiri, A. Brik and D. Shabat, *Bioconjugate Chem.*, 2021, **32**, 2141–2147.

37 J. I. Scott, S. Gutkin, O. Green, E. J. Thompson, T. Kitamura, D. Shabat and M. Vendrell, *Angew. Chem., Int. Ed.*, 2021, **60**, 5699–5703.

38 C. Peukert, S. P. Gholap, O. Green, L. Pinkert, J. van den Heuvel, M. van Ham, D. Shabat and M. Bronstrup, *Angew. Chem., Int. Ed.*, 2022, **61**, e202201423.

39 O. Shelef, S. Gutkin, D. Feder, A. Ben-Bassat, M. Mandelboim, Y. Haitin, N. Ben-Tal, E. Bacharach and D. Shabat, *Chem. Sci.*, 2022, **13**, 12348–12357.

40 S. Ye, B. W. Yang, M. L. Wu, Z. F. Chen, J. G. Shen, D. Shabat and D. Yang, *CCS Chem.*, 2022, **4**, 1871–1878.

41 M. David, Q. Jaber, M. Fridman and D. Shabat, *Chem.–Eur. J.*, 2023, e202300422.

42 J. S. Huang, Y. Y. Jiang, J. C. Li, J. G. Huang and K. Y. Pu, *Angew. Chem., Int. Ed.*, 2021, **60**, 3999–4003.

43 E. M. Digby, M. T. Tung, H. N. Kagalwala, L. S. Ryan, A. R. Lippert and A. A. Beharry, *ACS Chem. Biol.*, 2022, **17**, 1996.

44 H. N. Kagalwala, J. Gerberich, C. J. Smith, R. P. Mason and A. R. Lippert, *Angew. Chem., Int. Ed.*, 2022, **61**, e202115704.

45 H. N. Kagalwala, R. T. Reeves and A. R. Lippert, *Curr. Opin. Chem. Biol.*, 2022, **68**, 102134.

46 X. Wei, J. S. Huang, C. Zhang, C. Xu, K. Y. Pu and Y. Zhang, *Angew. Chem., Int. Ed.*, 2023, **62**, e202213791.

47 J. S. Huang, C. Zhang, X. Z. Wang, X. Wei and K. Y. Pu, *Angew. Chem., Int. Ed.*, 2023, e202303982.

48 J. S. Huang, P. H. Cheng, C. Xu, S. S. Liew, S. S. He, Y. Zhang and K. Y. Pu, *Angew. Chem., Int. Ed.*, 2022, **61**, e202203235.

49 N. Hananya, J. P. Reid, O. Green, M. S. Sigman and D. Shabat, *Chem. Sci.*, 2019, **10**, 1380–1385.

50 H. A. Ergen, U. Gormus, F. Narter, U. Zeybek, S. Bulgurcuoglu and T. Isbir, *Anticancer Res.*, 2007, **27**, 4107–4110.

51 J. M. Kolesar, S. E. Dahlberg, S. Marsh, H. L. McLeod, D. H. Johnson, S. M. Keller and J. H. Schiller, *Oncol. Rep.*, 2011, **25**, 1765–1772.

52 S. K. Beaver, N. Mesa-Torres, A. L. Pey and D. J. Timson, *Biochim. Biophys. Acta, Proteins Proteomics*, 2019, **1867**, 663–676.